J. Fluid Mech. (2010), *vol.* 643, *pp.* 33–58.
doi:10.1017/S0022112009991923

Short and long waves over a muddy seabed

CHIANG C. MEI[1]†, MIKHAEL KROTOV[2], ZHENHUA HUANG[3] AND AODE HUHE[4]

[1]Department of Civil and Environmental Engineering, Massachusetts Institute of Technology, Cambridge, MA 02139, USA

[2]Department of Aeronautics and Astronautics, Massachusetts Institute of Technology Cambridge, MA 02139, USA

[3]Department of Civil and Environmental Engineering, Nanyang Technological University, 50, Nanyang Avenue 639798, Singapore

[4]Institute of Mechanics, Chinese Academy of Sciences, Haidian District 100080, Beijing, China

(Received 4 May 2009; revised 1 September 2009; accepted 2 September 2009)

The available experimental results have shown that in time-periodic motion the rheology of fluid mud displays complex viscoelastic behaviour. Based on the measured rheology of fluid mud from two field sites, we study the interaction of water waves and fluid mud by a two-layered model in which the water above is assumed to be inviscid and the mud below is viscoelastic. As the fluid-mud layer in shallow seas is usually much thinner than the water layer above, the sharp contrast of scales enables an approximate analytical theory for the interaction between fluid mud and small-amplitude waves with a narrow frequency band. It is shown that at the leading order and within a short distance of a few wavelengths, wave pressure from above forces mud motion below. Over a much longer distance, waves are modified by the accumulative dissipation in mud. At the next order, infragravity waves owing to convective inertia (or radiation stresses) are affected indirectly by mud motion through the slow modulation of the short waves. Quantitative predictions are made for mud samples of several concentrations and from two different field sites.

Key words: coastal engineering, surface gravity waves, viscoelasticity

1. Introduction

Fluid mud is a mixture of water and highly cohesive clay particles often transported from inland rivers into the estuary and then deposited along the coast. Its motion changes the seabed, affects the wave climate and shapes the coastline in the long run. The problem of wave–mud interaction has been treated by considering a two-layered system in which water and mud are assumed to be Newtonian fluids with vastly different viscosities (Dalrymple & Liu 1978; Liu & Chan 2007). For monochromatic waves of infinitesimal amplitudes, the linearized problem is solved to obtain the dispersion relation between wavenumber k and frequency ω. For the general depth ratio the complex wavenumber is solved numerically. The imaginary part of k then gives the rate of spatial attenuation. Mud has also been modelled as a Kelvin–Voigt viscoelastic body by MacPherson (1980), Hsiao & Shemdin (1980) and Maa & Mehta (1988), where the coefficients of viscosity and elasticity are assumed to be constants. Second-order theories on the mass transport in fluid mud have been reported by

† Email address for correspondence: ccmei@mit.edu

Shibayama, Okuno & Sato (1990), Foda, Hunt & Chou (1993) and Piedra-Cueva. Recently Zhang & Ng (2006) and Ng & Zhang (2007) further hypothesized a nonlinear constitutive relation accounting for finite strain.

Owing to the importance of fluid mud in river hydraulics, abundant data exist for steady flow conditions under which mud rheology is essentially Bingham plastic (Wan & Wan 1994; Coussot 1997). Earlier theories are based on the assumption that fluid mud is either Newtonian (Dalrymple & Liu 1978) or Bingham plastic (Liu & Mei 1989). Experimental data for mud in periodic or transient motion are much scarcer in the published literature. With samples taken from different sites (Kerala coast of Southern India, Okeechobee Lake in Florida and Mobile Bay in Alabama) as well as from laboratory mixtures of attapulgite and kaolinite, Jiang & Mehta (1995) have found the stress–strain relation for simple harmonic motion to be distinctly viscoelastic. When fitted to a three-parameter Voigt model, the coefficients of elasticity and viscosity are functions not only of the solid concentration but also of wave frequency. Independent tests have also been performed by two of the present authors for both steady and periodic flows, using field samples from two different sites along the eastern coast of China, namely Hangzhou Bay of Zhejiang Province (Huhe & Huang 1994) and Lianyungang of Jiangsu Province (Huang, Huhe & Zhang 1992). The measured results for periodic flows are consistent with those of Jiang & Mehta (1995). Since the range of frequencies in their tests coincides with those of sea waves, their findings are considered to be the relevant basis for coastal studies.

In this paper, we shall investigate wave–mud interaction with an emphasis on the fate of waves. Fluid mud is modelled as a viscoelastic material. The primary waves will be assumed to be nearly sinusoidal with long-scale modulation because of a small frequency spread. Attenuation and wavenumber shift in the primary waves will be deduced first by a multiple-scale perturbation analysis. Infragavity waves forced by radiation stresses will then be found at the next order. In line with available experimental data, water is assumed to be inviscid, since the viscosity is typically 10^3 Pa s for fluid mud and 10^{-3} Pa s for pure water. Interfacial mixing is also ignored. Mud is assumed to be linearly viscoelastic. The characteristic wave amplitude a_0, and hence the vertical displacement at the water–air interface η, will be assumed to be small compared with the water depth h or the wavelength $\lambda = 2\pi/k$:

$$\eta = O(a_0), \quad k\eta = O(ka_0) = O(\epsilon) \ll 1. \tag{1.1}$$

Referring to figure 1, we shall consider the water depth h to be constant and comparable to the wavelength so that $kh = O(1)$. The fluid-mud depth d is also assumed to be constant over a region greater than the attenuation distance to be defined later. In coastal waters the typical mud depth d is usually below $O(0.5\,\mathrm{m})$ and much smaller than the depth of water h above so that

$$\frac{d}{h} = O(\epsilon) \ll 1. \tag{1.2}$$

As a consequence Liu & Mei (1989) showed that the vertical displacement of the mud–water interface, ζ, is much smaller than that of the free surface:

$$k\zeta \sim O(\epsilon^2) \ll 1 \quad \text{or} \quad \zeta = O(\epsilon\eta). \tag{1.3}$$

This fact has been employed in Ng (2000) to simplify the full dispersion relation of two layers of Newtonian viscous fluids. Taking advantage of this disparity, we shall use a multiple-scale perturbation analysis to further reduce the approximate analysis in order to reveal the physics for a viscoelastic mud. In particular at the leading order

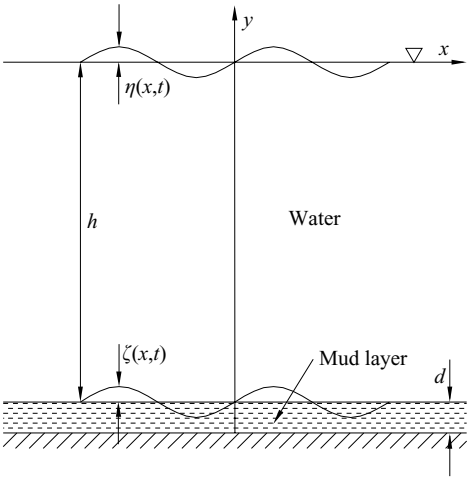

FIGURE 1. A thin mud layer over seabed.

in wave steepness, mud is forced to move passively by the hydrodynamic pressure from the surface waves above, resulting in viscous dissipation within. Over very long distance, mud dissipation gradually alters the leading-order waves above by creating a complex shift of wavenumber, which amounts to attenuation of wave amplitude and change of wavelength. Also at the second-order, long-scale modulation of the mud-affected primary waves leads to set-down and infragravity waves which are indirectly affected by mud. Quantitative predictions for different mud samples of contrasting properties are moreover examined in the paper.

2. Dynamic rheology of fluid mud

We present in this section some data on dynamic rheology of fluid mud from Hangzhou Bay of Zhejiang Province (Huhe & Huang 1994) and Lianyungang Harbour of Jiangshu Province (Huang *et al.* 1992) on the eastern coast of China. To achieve a range of concentrations, the field samples were mixed with salt water having a salinity of 0.15 %. Dynamic measurements were made for a broad range of frequencies by using a strain-controlled rotary shear rheometer (Model RMS-605, Rheometrics Mechanical Spectrometer, Piscataway, NJ). The temperature maintained was 15°C during the measurements.

For a mud sample of bulk density $\rho^{(m)}$, the volume concentration ϕ can be calculated from $\rho^{(m)} = \phi\rho^{(s)} + (1-\phi)\rho^{(w)}$, where $\rho^{(s)}$ is the mineral density (grain density) and ρ_w the density of water. The Hangzhou Bay mud is made of relatively coarse sediments with $D_{50} = 90\,\mu\text{m}$. The grain density is $\rho^{(s)} = 2650\,\text{kg m}^{-3}$, and the bulk density of the natural mud sample is $\rho^{(m)} = 1670\,\text{kg m}^{-3}$. In the rheology measurements, volume concentrations of solid varied from $\phi = 0.02$ to $\phi = 0.34$, corresponding to the bulk density range of $\rho^{(m)} = 1048$–$1670\,\text{kg m}^{-3}$. The Lianyungang Harbour mud is very fine with $D_{37} = 5\,\mu\text{m}$, $D_{85} = 50\,\mu\text{m}$. The grain density $\rho^{(s)} = 2750\,\text{kg m}^{-3}$, and the bulk density of natural mud $\rho^{(m)} = 1720\,\text{kg m}^{-3}$. Again by mixing with salt water, volume concentrations ranging from $\phi = 0.06$ to $\phi = 0.50$ were generated, corresponding to the bulk density range of $\rho^{(m)} = 1100$–$1590\,\text{kg m}^{-3}$. Other information on Hangzhou Bay mud and Lianyungang mud can be found in Huang *et al.* (1992) and Huhe & Huang (1994).

For steady unidirectional mud flows the stress–strain relation was found to be essentially Bingham plastic, in accord with nearly all past experiments. However for time-harmonic tests within the frequency range $0.1 < \omega < 70\,\mathrm{rad\,s^{-1}}$, the relation was decidedly viscoelastic. The data were originally fitted to a simple Kelvin–Voigt relation between shear stress τ' and strain rate $\partial \mathscr{E}'/\partial t$,

$$\tau' = \left(\mu_m + \frac{\mathrm{i}G_m}{\omega}\right)\frac{\partial \mathscr{E}'}{\partial t'}, \tag{2.1}$$

where $\mathscr{E}' = \partial U'/\partial y'$ and U' represents the time-harmonic fluid displacement. All physical variables are distinguished by primes. The coefficients G_m and μ_m were found to depend not only on mud properties (chemistry, salinity, density and sediment concentration and the like) but also strongly on the frequency. Specifically, the shear modulus G_m increased, while the viscosity coefficient μ_m decreased with increasing frequency. The range of frequencies in both studies coincides with the common range of sea waves and hence is of direct relevance to coastal/ocean engineering.

For analysing general transient or nonlinear problems, it is desirable to express the constitutive relation in the generalized form (Malvern 1969),

$$\sum_{n=0}^{N} \alpha_n \frac{\partial^n \tau'_{ij}}{\partial t'^n} = \sum_{n=0}^{N} \beta_n \frac{\partial^n \mathscr{E}'_{ij}}{\partial t'^n}, \tag{2.2}$$

so that the real coefficients (α_n, β_n) depend only on material properties but not on the frequency. For applications to linearized problems of monochromatic waves, this representation is in principle not necessary. It suffices to express the stress–strain relation formally in the Newtonian form,

$$\tau' = \mu_d(\omega)\frac{\partial \mathscr{E}'}{\partial t'}, \tag{2.3}$$

where

$$\mu_d(\omega) = \mathrm{Re}(\mu_d(\omega)) + \mathrm{iIm}(\mu_d(\omega)) = |\mu_d(\omega)|\,\mathrm{e}^{\mathrm{i}\theta(\omega)} \tag{2.4}$$

is the complex viscosity depending on frequency. We have converted the discrete data for the mud from Hangzhou Bay and Liangyungang into the form of (2.2) in order to obtain μ_d for a continuous range of frequencies. For the later purpose of scaling we define μ_0 to be the real part of μ_d extrapolated at $\omega = 0$, i.e.

$$\mu_0 \equiv \mathrm{Re}(\mu_d|_{\omega=0}). \tag{2.5}$$

From the converted Hangzhou Bay data, the magnitude and phase of μ_d are shown as functions of frequency in figure 2, where the fitted curves are determined by truncating (2.2) with only four pair of coefficients and matching data at four different frequencies in the range $0.1 < \omega < 10\,\mathrm{rad\,s^{-1}}$, which are of interest for wind waves in nature. Note that the phase angle θ is not close to $\pi/2$; hence Hangzhou Bay mud is closer in character to a viscous fluid than an elastic solid.

Similar conversion of Lianyungang data is shown in figure 3. Note that the magnitudes of the complex viscosity of Lianyungang mud samples are considerably higher than those of Hangzhou Bay mud. Note further that θ is closer to $\pi/2$; hence the fine particles in Lianyungang mud increase the elasticity of the mixture, unlike the mud in Hangzhou Bay but similar to the Mobile Bay data of Jiang & Mehta (1995).

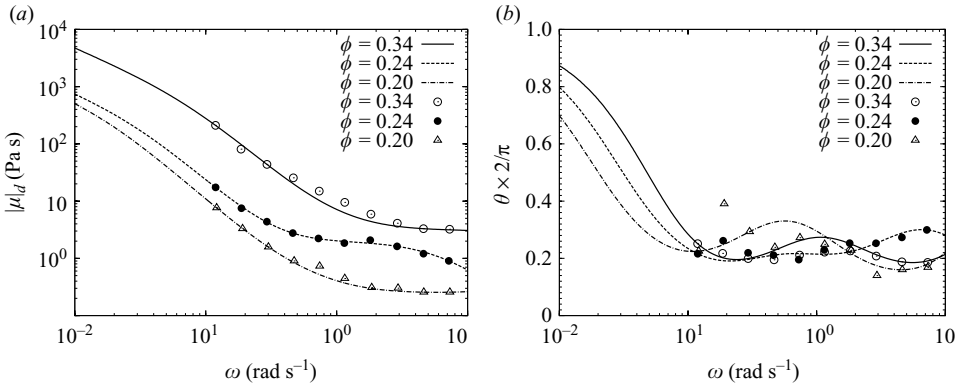

FIGURE 2. (*a*) Magnitude and (*b*) phase of complex viscosity of mud samples from East Pilot Navigation Channel, Hangzhou Bay: symbols, data; lines, fitted curve by generalized viscoelastic model.

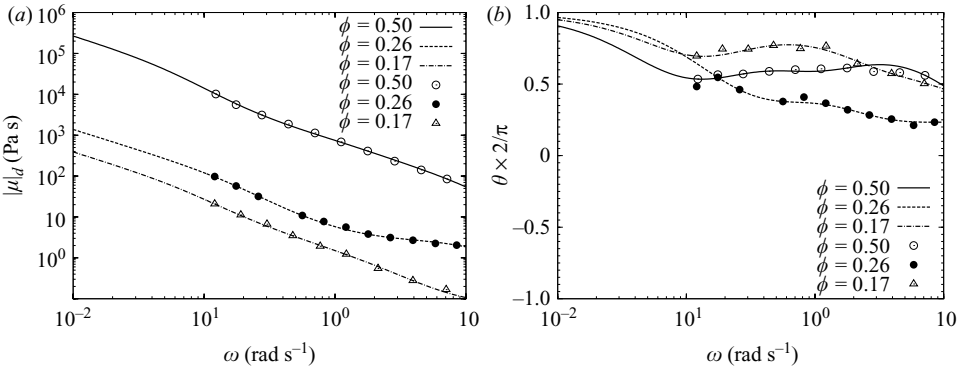

FIGURE 3. (*a*) Magnitude and (*b*) phase of complex viscosity of mud samples from Lianyungang: symbols, data; lines, fitted curve by generalized viscoelastic model.

Within the frequency range of coastal interest, however, none of the field samples is strictly viscous or elastic.

3. Theoretical formulation

3.1. *Dimensionless conservation laws*

We consider a water layer of constant mean depth h over a shallow layer of fluid mud with depth $d \ll h$. Long-crested progressive surface waves propagate in the positive x'- direction. Let rectangular coordinates x', y' be used to describe a vertical plane with its origin on the mean sea surface, as sketched in figure 1. Primes are used to distinguish all dimensional variables from their dimensionless counterparts.

Let Φ' denote the velocity potential in the inviscid water layer and η' the free-surface displacement. In the fluid-mud layer below, u', v' are the velocity components and ζ' is the interface displacement. The viscoelastic stress and strain tensors in mud are denoted by τ'_{ij} and $\mathscr{E}'_{ij}$. Finally $(p^{(w)'}, p^{(m)'})$ and $(\rho^{(w)}, \rho^{(m)})$ denote the dynamic pressure and density, with the superscripts w and m indicating water and mud,

respectively. The static and total pressures will be denoted by p'_s and P', respectively, with $P' = p'_s + p'$. In addition, the total stress will be denoted by $T'_{ij} = -P'\delta_{ij} + \tau'_{ij}$.

Let ω and a_0 be the frequency and the reference amplitude of the surface waves. For the water layer the following normalization is used:

$$(x', y', h) = \frac{g}{\omega^2}(x, y, H), \quad t' = \omega^{-1}t, \quad k' = \frac{\omega^2}{g}k,$$
$$\Phi' = \frac{a_0 g}{\omega}\Phi, \quad \eta' = a_0\eta, \quad \left(P^{(w)'}, p^{(w)'}\right) = \rho^{(w)} g a_0 \left(P^{(w)}, p^{(w)}\right). \quad (3.1)$$

We have chosen the deep-water wavelength g/ω^2 as the principal length scale for the purpose of examining the effects of varying depths of water. In dimensionless variables (without primes) the velocity potential is governed by

$$\frac{\partial^2\Phi}{\partial x^2} + \frac{\partial^2\Phi}{\partial y^2} = 0. \quad (3.2)$$

Let us define

$$\epsilon = \frac{\omega^2 a_0}{g} \ll 1, \quad (3.3)$$

which is a small parameter characterizing the wave slope. In dimensionless form, the total pressure $P^{(w)}$ in water is related to Φ by Bernoulli's equation,

$$-P^{(w)} = -p_s^{(w)} - p^{(w)} = \frac{y}{\epsilon} + \frac{\partial\Phi}{\partial t} + \frac{\epsilon}{2}\left[\left(\frac{\partial\Phi}{\partial x}\right)^2 + \left(\frac{\partial\Phi}{\partial y}\right)^2\right], \quad (3.4)$$

where $p_s^{(w)} = y/\epsilon$ and $p^{(w)}$ are the static and dynamic pressures, respectively.

For the mud layer, a new vertical coordinate measured from the mud bottom is introduced,

$$Y' = y' + h + d. \quad (3.5)$$

The total stress $\boldsymbol{T}'_{ij}$ is related to the mud pressure $P^{(m)'}$ and viscoelastic stress τ'_{ij} by

$$\boldsymbol{T}'_{ij} = -\left(p_s^{(m)'} + p^{(m)'}\right)\boldsymbol{\delta}_{ij} + \boldsymbol{\tau}'_{ij}, \quad (3.6)$$

where

$$p_s^{(m)'} = \rho^{(w)} g h - \rho^{(m)} g(h + y') = \rho^{(w)} g h + \rho^{(m)} g(d - Y') \quad (3.7)$$

is the hydrostatic pressure and $p^{(m)'}$ the hydrodynamic pressure. We further assume that the mud depth d is comparable to the wave amplitude a_0, i.e.

$$d/a_0 = O(1), \quad a_0/h = O(d/h) = O(\epsilon) \ll 1, \quad (3.8)$$

and define the dimensionless variables as follows:

$$\left.\begin{aligned} &x' = \frac{g}{\omega^2}x, \quad Y' = dY \quad t' = \omega^{-1}t, \quad \zeta' = \epsilon a_0\zeta, \\ &u' = a_0\omega\, u, \quad v' = \left(\epsilon a_0\omega\frac{d}{a_0}\right)v, \quad (p', P') = \left(\gamma\rho^{(m)} g a_0\right)\left(p^{(m)}, P^{(m)}\right), \\ &\boldsymbol{T}'_{ij} = \left(\gamma\rho^{(m)} g a_0\right)\boldsymbol{T}_{ij}, \quad \boldsymbol{\tau}'_{ij} = \frac{\mu_0\omega a_0}{d}\boldsymbol{\tau}_{ij}, \quad \dot{\boldsymbol{E}}'_{ij} = \frac{\omega a_0}{d}\dot{\boldsymbol{E}}_{ij}, \end{aligned}\right\} \quad (3.9)$$

where $\gamma = \rho^{(m)}/\rho^{(w)}$ is the ratio of mud density to water density and μ_0 is defined in (2.5). Note that the same stress scale is used in both water and mud. Inside the mud

layer, $0 < Y < 1$, and mass conservation requires that

$$\frac{\partial u}{\partial x} + \frac{\partial v}{\partial Y} = 0. \tag{3.10}$$

The dimensionless momentum equations read

$$\frac{\partial u}{\partial t} + \epsilon\left(u\frac{\partial u}{\partial x} + v\frac{\partial u}{\partial Y}\right) = -\gamma\frac{\partial p^{(m)}}{\partial x} + \frac{1}{Re}\frac{a_0}{d}\left(\frac{\partial \boldsymbol{\tau}_{xy}}{\partial Y} + \epsilon\frac{d}{a_0}\frac{\partial \boldsymbol{\tau}_{xx}}{\partial x}\right) \tag{3.11}$$

and

$$\left(\epsilon\frac{d}{a_0}\right)^2\left[\frac{\partial v}{\partial t} + \epsilon\left(u\frac{\partial v}{\partial x} + v\frac{\partial v}{\partial Y}\right)\right] = -\gamma\frac{\partial p^{(m)}}{\partial Y} + \frac{\epsilon}{Re}\left(\frac{\partial \boldsymbol{\tau}_{yy}}{\partial Y} + \epsilon\frac{d}{a_0}\frac{\partial \boldsymbol{\tau}_{xy}}{\partial x}\right), \tag{3.12}$$

where Re denotes the characteristic Reynolds number defined by the characteristic viscosity in (2.5),

$$Re = \frac{\rho^{(m)} a_0 \omega d}{\mu_0}. \tag{3.13}$$

As a rough estimate we take $\rho^{(m)} = 1600\,\mathrm{kg\,m^{-3}}$, $a_0 = d = 1$ m, $\omega = 0.5\,\mathrm{rad\,s^{-1}}$ and $\mu_0 = 10^3$–$10^4\,\mathrm{Pa\,s} = 10^3$–$10^4\,\mathrm{N\,s\,m^{-2}}$; then $Re = 0.08$–0.8, which will be regarded as being of order unity. Hence viscous effects throughout the mud layer must be treated without the boundary-layer approximation.

In dimensionless form, the total stress (static and dynamic) is

$$\boldsymbol{T}_{ij} = -\left(p_s^{(m)} + p^{(m)}\right)\boldsymbol{\delta}_{ij} + \frac{\epsilon}{\gamma Re}\boldsymbol{\tau}_{ij}, \tag{3.14}$$

where

$$p_s^{(m)} = \frac{H}{\epsilon} + \gamma(1 - Y). \tag{3.15}$$

Finally the dimensionless strain tensor is given by

$$\{\boldsymbol{E}_{ij}\} = \begin{pmatrix} \boldsymbol{E}_{xx} & \boldsymbol{E}_{xy} \\ \boldsymbol{E}_{yx} & \boldsymbol{E}_{yy} \end{pmatrix} = \begin{pmatrix} 2\epsilon\dfrac{d}{a_0}\dfrac{\partial U}{\partial x} & \dfrac{\partial U}{\partial Y} + \left(\epsilon\dfrac{d}{a_0}\right)^2\dfrac{\partial V}{\partial x} \\ \dfrac{\partial U}{\partial Y} + \left(\epsilon\dfrac{d}{a_0}\right)^2\dfrac{\partial V}{\partial x} & 2\epsilon\dfrac{d}{a_0}\dfrac{\partial V}{\partial Y} \end{pmatrix}.$$

3.2. *Dimensionless boundary conditions*

On the free surface S_F of water we impose the kinematic condition that the flow can only be tangential:

$$\frac{\partial \eta}{\partial t} = \frac{\partial \Phi}{\partial y} - \epsilon\frac{\partial \eta}{\partial x}\frac{\partial \Phi}{\partial x}, \quad y = \epsilon\eta. \tag{3.16}$$

Assuming uniform atmospheric pressure, the dynamic boundary condition is

$$-\eta = \frac{\partial \Phi}{\partial t} + \frac{\epsilon}{2}\left[\left(\frac{\partial \Phi}{\partial x}\right)^2 + \left(\frac{\partial \Phi}{\partial y}\right)^2\right], \quad y = \epsilon\eta. \tag{3.17}$$

The two conditions above can be combined to give

$$\Gamma\Phi + \epsilon\left[\frac{\partial}{\partial t} + \frac{\epsilon}{2}\left(\frac{\partial \Phi}{\partial x}\frac{\partial}{\partial x} + \frac{\partial \Phi}{\partial y}\frac{\partial}{\partial y}\right)\right]\left[\left(\frac{\partial \Phi}{\partial x}\right)^2 + \left(\frac{\partial \Phi}{\partial y}\right)^2\right] = 0, \quad y = \epsilon\eta, \tag{3.18}$$

where Γ denotes the differential operator

$$\Gamma = \frac{\partial^2}{\partial t^2} + \frac{\partial}{\partial y}. \tag{3.19}$$

On the mud–water interface S_I is described equivalently by

$$Y = 1 + \epsilon \frac{a_0}{d}\zeta, \quad \text{or} \quad y = -H + \epsilon^2 \zeta, \tag{3.20}$$

where H is the normalized water depth; the kinematic condition is

$$\frac{\partial \Phi}{\partial y} = \epsilon \frac{\partial \zeta}{\partial t} + \epsilon^2 \frac{\partial \zeta}{\partial x}\frac{\partial \Phi}{\partial x}, \quad y = -H + \epsilon^2 \zeta, \tag{3.21}$$

for water, and

$$\frac{\partial \zeta}{\partial t} = \frac{d_0}{a_0} v - \epsilon u \frac{\partial \zeta}{\partial x}, \quad Y = 1 + \epsilon \frac{a_0}{d_0}\zeta, \tag{3.22}$$

for mud. Continuity of total (hydrostatic and dynamic) stress on the mud–water interface then requires

$$\boldsymbol{T}_{xx} n_x + \boldsymbol{T}_{xy} n_y = -\left(p_s^{(w)} + p^{(w)}\right) n_x, \tag{3.23}$$

$$\boldsymbol{T}_{yx} n_x + \boldsymbol{T}_{yy} n_y = -\left(p_s^{(w)} + p^{(w)}\right) n_y \tag{3.24}$$

on $Y = 1 + \epsilon(a_0/d)\zeta$ (or equivalently $y = -H + \epsilon^2\zeta$). The components of the unit normal are

$$n_x = \frac{\epsilon^2 \dfrac{d}{a_0}\dfrac{\partial \zeta}{\partial x}}{\sqrt{1 + \epsilon^4 \left(\dfrac{d}{a_0}\dfrac{\partial \zeta}{\partial x}\right)^2}}, \quad n_y = \frac{1}{\sqrt{1 + \epsilon^4 \left(\dfrac{d}{a_0}\dfrac{\partial \zeta}{\partial x}\right)^2}}. \tag{3.25}$$

At the bottom of the mud layer, we impose the following no-slip condition:

$$u = v = 0, \quad y' = 0. \tag{3.26}$$

4. Multiple-scale analysis

For small-amplitude waves, it is natural to employ the asymptotic method of perturbations. Anticipating that damping will become significant only after a very long distance and that the waves may have a narrow frequency band and hence a long time scale inversely proportional to the bandwidth, we define the following multiple-scale coordinates in terms of ϵ:

$$x, \; x_1 = \epsilon x, \quad t, \; t_1 = \epsilon t. \tag{4.1}$$

Each of the unknowns $\mathscr{F}$, which may represent $\zeta, \eta, \Phi, u, v, \ldots$, will be expanded as power series,

$$\mathscr{F} = \mathscr{F}_0 + \epsilon \mathscr{F}_1 + \epsilon^2 \mathscr{F}_2 + \ldots, \tag{4.2}$$

where (η_n, ζ_n) depend on $(x, x_1; t, t_1)$ only, Φ_n on $(x, x_1; y; t, t_1)$ in water and (u_n, v_n) on $(x, x_1; Y; t, t_1)$ in fluid mud. Expansions of the form of (4.2) are first substituted into all conservation laws, yielding perturbation equations after separating the orders. On either the free surface or the interface, the boundary conditions are first Taylor-expanded about the static levels, which are $y = 0$ for the free surface and $y = -H$ or

$y' = 1$ for the mud–water interface. Then the multi-scale series are substituted into the results to give perturbation boundary conditions at separate orders.

5. Perturbation problems in water

We consider the surface waves to be narrow-banded, i.e. nearly simple harmonic with slowly varying amplitude,

$$\eta = \eta_0 + O(\epsilon) = \frac{1}{2} A(x_1, t_1)\, e^{i\psi} + \text{c.c.} + O(\epsilon), \tag{5.1}$$

where $A(x_1, t_1)$ is the slowly varying amplitude and

$$\psi = k_0 x - t \tag{5.2}$$

is the phase of the carrier waves. The perturbation unknowns at order n are then expressed in sums of harmonics up to $\pm n$,

$$\mathscr{F}_n = \sum_{m=-n}^{n} \mathscr{F}_{nm} e^{im\psi}. \tag{5.3}$$

After separating orders and harmonics, the boundary value problem for each index pair (n, m) is then obtained.

The analysis of the potential in water is standard and similar to that for waves over a rigid bed (see, e.g., Mei 1989). Omitting the details we only cite the key results here. The fast variations of the perturbation potentials Φ_{nm} are governed by the following boundary value problems. In particular, Laplace's equation gives

$$\frac{\partial^2 \Phi_{nm}}{\partial y^2} - m^2 k_0^2 \Phi_{nm} = F_{nm}, \quad n = 0, 1, 2, \ldots, \quad m = 0, \pm 1, \ldots, \pm n, -H < y < 0. \tag{5.4}$$

On the free surface the combined kinematic and dynamic conditions gives

$$\frac{\partial \Phi_{nm}}{\partial y} - m^2 \Phi_{nm} = G_{nm}, \quad n = 0, 1, 2, \quad m = 0, \pm 1, \ldots, \pm n, \quad y = 0. \tag{5.5}$$

The forcing terms F_{nm} and G_{nm} are known from harmonics of orders lower than $\pm n$ and are the same as those for a rigid seabed (see Mei 1989). In particular

$$F_{00} = F_{01} = 0, \quad G_{00} = G_{01} = 0. \tag{5.6}$$

On the water–mud interface, the kinematic boundary condition gives

$$\frac{\partial \Phi_{nm}}{\partial y} = L_{nm}, \quad n = 0, 1, 2, \quad m = 0, \pm 1, \ldots, \pm n, \quad y = -H, \tag{5.7}$$

where L_{nm} are the results of small vertical displacement of the water–mud interface. However, at the leading order $L_{00} = L_{01} = 0$. Results at higher orders ($n = 1, 2, \ldots$) will be given later.

Since at the leading order ($n = 0$) the boundary value problems for both Φ_{00} and Φ_{01} are homogeneous, the solutions describing the fast variations are simple. The zeroth harmonic is

$$\Phi_{00} = \Phi_{00}(x_1, t_1), \tag{5.8}$$

which represents long waves. For the first harmonic Φ_{01} we take a plane progressive wave corresponding to (5.1),

$$\Phi_{01} = -\frac{\mathrm{i}A}{2}\frac{\cosh Q}{\cosh q}, \quad \text{where} \quad Q \equiv k_0(y+H), \quad q \equiv k_0 H, \tag{5.9}$$

and k_0 satisfies the dispersion relation,

$$k_0 \tanh k_0 H = 1. \tag{5.10}$$

The dependence of $A(x_1, t_1)$, $\Phi_{00}(x_1, t_1)$ on slow coordinates is yet to be found.

At higher orders the problems for the potentials of these two harmonics are in general inhomogeneous and hence must be subjected to solvability conditions. For $\Phi_{n0}, n = 1, 2, \ldots,$ we integrate the governing equations from $y = -H$ to $y = 0$ and apply the boundary conditions to get

$$\int_{-H}^{0} \mathrm{d}y F_{n0} = G_{n0} - L_{n0}, \quad n = 1, 2, \ldots . \tag{5.11}$$

For Φ_{n1} we apply Green's formula to the governing conditions for Φ_{01} and Φ_{n1} and get

$$\int_{-H}^{0} \mathrm{d}y F_{n1}\frac{\cosh Q}{\cosh q} = G_{n1} - L_{n1}, \quad n = 1, 2, \ldots . \tag{5.12}$$

We shall seek the evolution equations for the short-wave envelope ($A(x_1, t_1)$) and the long-wave potential ($\Phi_{00}(x_1, t_1)$). As in the simpler case of pure water over a rigid bed (see Mei 1989), the first and second solutions are found respectively from the solvability conditions of $\epsilon\Phi_{11}$ and $\epsilon^2\Phi_{20}$. The seemingly complex analysis of mud motion can be in part lessened by the fact that the solvability of Φ_{11} depends only on ζ_{01} through the kinematic condition on the mud–water interface. Similarly it will be shown shortly that the solvability of Φ_{20} depends also on the mud dynamics $O(1)$. Hence there is no need to go to the higher-order analysis of mud unless its nonlinear physics such as induced streaming is wanted.

6. Mud motion at the leading order

Since there is no forcing pressure at the long scale from water at $O(1)$, mud response is limited to short scales and to the first harmonic,

$$\left(u_0, v_0, p^{(m)}\right) = \left(u_{01}, v_{01}, p_{01}^{(m)}\right)\mathrm{e}^{\mathrm{i}\psi} + \text{c.c.}, \quad 0 < Y < 1. \tag{6.1}$$

Since there is no zeroth-harmonic forcing from above at this order, we have

$$p_{00}^{(w)} = 0 \quad \text{and} \quad u_{00} = v_{00} = \zeta_{00} = 0, \quad 0 < y' < 1. \tag{6.2}$$

The problem for the first-harmonic amplitude u_{01} is similar to that of Stokes oscillatory boundary layer. Mass conservation requires

$$\frac{\partial v_{01}}{\partial Y} + \mathrm{i}k_0 u_{01} = 0, \quad 0 < y' < 1. \tag{6.3}$$

The constitutive relation reduces to

$$(\boldsymbol{\tau}_{ij})_{01} = \mu(\omega)(\dot{\boldsymbol{E}}_{ij})_{01}, \quad \text{where} \quad (\dot{\boldsymbol{E}}_{ij})_{01} = \begin{pmatrix} 0 & \dfrac{\partial u_{01}}{\partial Y} \\ \dfrac{\partial u_{01}}{\partial Y} & 0 \end{pmatrix}$$

and

$$\mu(\omega) \equiv \mu_d/\mu_0 \tag{6.4}$$

is the dimensionless complex viscosity. Momentum conservation requires

$$-iu_{01} = -\mathrm{i}k_0\gamma p_{01}^{(w)} + \frac{\mu}{Re}\frac{a_0}{d}\frac{\partial^2 u_{01}}{\partial Y^2}, \quad 0 < Y < 1, \tag{6.5}$$

$$\frac{\partial p_{01}^{(m)}}{\partial Y} = 0, \quad 0 < Y < 1. \tag{6.6}$$

On the water–mud interface the dynamic boundary conditions are

$$\mu\frac{\partial u_{01}}{\partial Y} = 0, \quad Y = 1, \tag{6.7}$$

$$p_{01}^{(m)}|_{Y=1} = p_{01}^{(m)}|_{y=-H} = \frac{A}{2\cosh q}. \tag{6.8}$$

The hydrostatic pressure on the interface is $p_s^{(m)} = H/\epsilon + \gamma\epsilon\zeta$, which is essentially uniform and has no dynamic influence. On the mud bottom we have

$$u_{01} = v_{01} = 0, \qquad Y = 0. \tag{6.9}$$

Thus mud is forced to move only passively by the dynamic pressure from above.

Equation (6.5) can be written as

$$\frac{\partial^2 u_{01}}{\partial Y^2} - \sigma^2 u_{01} = -\sigma^2\frac{k_0\gamma A}{2\cosh q}, \tag{6.10}$$

where

$$\sigma^2 \equiv -\mathrm{i}\frac{Re}{\mu}\frac{d}{a_0}. \tag{6.11}$$

The solution to (6.7), (6.9) and (6.10) is easily found to be

$$u_{01}(Y) = \frac{\gamma k_0 A}{2\cosh q}\left[1 - \cosh(\sigma Y) + \tanh(\sigma)\sinh(\sigma Y)\right].$$

Integrating the mass conservation equation and using the no-slip boundary condition at the bottom we obtain the vertical velocity profile:

$$v_{01}(Y) = -\mathrm{i}\frac{\gamma k_0 A}{2\lambda_0\sinh q}[\sigma Y - \sinh(\sigma Y) + \tanh\sigma[\cosh(\sigma Y) - 1]]. \tag{6.12}$$

Finally, the amplitude of the interface displacement ζ_{01} follows from the kinematic boundary condition:

$$\zeta_{01} = \mathrm{i}\frac{d}{a_0}(v_{01})|_{Y=1} = \gamma\frac{d}{a_0}\frac{k_0 A}{2\sinh q}G(\sigma), \tag{6.13}$$

where

$$G(\sigma) = 1 - \frac{\tanh\sigma}{\sigma}. \tag{6.14}$$

The complex constant σ characterizes the fluid mud and depends on frequency. For later convenience we define the (dimensional) Stokes boundary-layer depth δ_S and the depth ratio D of the mud layer to the Stokes layer,

$$\delta_S \equiv \sqrt{\frac{2|\mu_d'|}{\rho^{(m)}\omega}}, \quad D \equiv \frac{d}{\delta_S}. \tag{6.15}$$

Since $\mu(\omega) = |\mu| e^{i\theta}$ we have

$$\sigma(D, \theta) = \sqrt{-i \frac{Re\, d}{\mu\, a_0}} = D\sqrt{2} e^{-i\left(\frac{\theta}{2}+\frac{\pi}{4}\right)} \equiv -i(\alpha + i\beta)D, \tag{6.16}$$

which defines the real coefficients α, β:

$$\alpha \equiv \sqrt{2} \sin\left(\frac{\theta}{2} + \frac{\pi}{4}\right), \quad \beta \equiv \sqrt{2} \cos\left(\frac{\theta}{2} + \frac{\pi}{4}\right). \tag{6.17}$$

As ω varies, the phase of σ is confined in the fourth quadrant of the complex plane since $0 < \theta < \pi/2$, and its amplitude increases with the depth ratio D, and hence with ω, and decreases with increasing μ.

7. Water motion at $O(\epsilon)$

The zeroth-harmonic problem is again homogeneous, governed by $\partial^2 \Phi_{10}/\partial y^2 = 0$ and subjected to the boundary conditions $\partial \Phi_{10}/\partial y = 0$ at $y = 0, 1$. Therefore, the potential depends only on the slow coordinates

$$\Phi_{10} = \Phi_{10}(x_1, t_1) \tag{7.1}$$

which can be absorbed in Φ_{00} and are omitted from here on. The corresponding hydrodynamic pressure and mean free-surface displacement are related to the long-wave potential Φ_{00}, which is yet unknown:

$$p_{10}^{(w)} = -\frac{\partial \Phi_{00}}{\partial t_1} - \frac{|A|^2}{4 \sinh^2 q} \cosh(2Q), \tag{7.2}$$

$$\eta_{10} = -\frac{\partial \Phi_{00}}{\partial t_1} - \frac{|A|^2}{4 \sinh^2 q}. \tag{7.3}$$

The first harmonic is governed by

$$\frac{\partial^2 \Phi_{11}}{\partial y^2} - k_0^2 \Phi_{11} = F_{11} = -2ik_0 \frac{\partial \Phi_{01}}{\partial x_1} = -k_0 \frac{\cosh Q}{\cosh q} \frac{\partial A}{\partial x_1} \tag{7.4}$$

and is subjected to the boundary conditions on the free surface:

$$\frac{\partial \Phi_{11}}{\partial y} - \Phi_{11} = G_{11} = \frac{\partial A}{\partial t_1}, \quad y = 0. \tag{7.5}$$

The potential now receives feedback from the displacement of the interface,

$$\frac{\partial \Phi_{11}}{\partial y} = L_{11} = -i\zeta_{01}, \quad y = -H \tag{7.6}$$

Invoking the solvability condition (5.11) and using (6.13) we arrive at the evolution equation of the free-surface wave amplitude A:

$$\frac{\partial A}{\partial t_1} + C_g \frac{\partial A}{\partial x_1} = ik_1 C_g A, \tag{7.7}$$

where

$$C_g = \frac{1}{2k_0}\left(1 + \frac{2q}{\sinh 2q}\right) \tag{7.8}$$

is the dimensionless group velocity. The right-hand side of (7.7) signifies the feedback from the mud layer on the long-scale variation of the leading-order wave. The complex shift of wavenumber k_1 is

$$k_1 = k_1^r + \mathrm{i}k_1^i = -\gamma \frac{d}{a_0}\left(\frac{2k_0^2}{2q + \sinh 2q}\right)(G(\sigma)). \tag{7.9}$$

Note from (6.13) that both ζ_{01} and k_1 depend on σ through the common factor $G(\sigma)$.

Now the first-harmonic problem can be explicitly solved to give

$$\Phi_{11} = \mathrm{i}k_1 C_g A \sinh q \sinh Q - \frac{Q \sinh Q}{2k_0 \cosh q}\frac{\partial A}{\partial x_1}, \tag{7.10}$$

$$p_{11}^{(w)} = \frac{\mathrm{i}}{2k_0 \cosh q}\left(k_0 \frac{\partial A}{\partial t_1}\cosh Q - A_{x_1} Q \sinh Q\right) - k_1 C_g A \sinh q \sinh Q, \tag{7.11}$$

$$\eta_{11} = \frac{\mathrm{i}}{2}\frac{\partial A}{\partial t_1} - k_1 C_g A \sinh^2 q - \mathrm{i}\frac{q \sinh q}{2k_0 \cosh q}\frac{\partial A}{\partial x_1}. \tag{7.12}$$

In the absence of the mud layer, $k_1 = 0$, and the solution reduces certainly to that for the inviscid water waves propagating over a solid bottom (Mei 1989).

The second-harmonic potential Φ_{12} is needed for examining the solvability of Φ_{20}. The governing equation in water and the free-surface conditions are no different from those for the case of pure water waves. In particular the kinematic condition on the interface $z = -H$ is $\partial\Phi_{12}/\partial z = 0$, since $\epsilon\zeta_0 = \epsilon\zeta_{01}\mathrm{e}^{-\mathrm{i}t} + \text{c.c.}$ consists of only the first harmonic. Hence the second-harmonic solutions are formally the same as those for a rigid bed (see Mei 1989) and are listed below for later reference:

$$\Phi_{12} = \frac{3\mathrm{i}}{16}\frac{A^2}{\sinh^4 q}\cosh 2Q, \tag{7.13}$$

$$p_{12}^{(w)} = -\frac{1}{8}\frac{1}{\sinh^2 q}A^2\left(1 + 3\frac{\cosh 2Q}{\sinh^2 q}\right), \tag{7.14}$$

$$\eta_{12} = \frac{A^2}{8}\frac{1}{\sinh^2 q}\left(2\sinh^2 q - 1 - \frac{3\mathrm{i}}{\sinh^2 q}\right). \tag{7.15}$$

8. Physics of the leading order

8.1. *Envelope of narrow-banded waves*

Let us consider a narrow-banded wavetrain entering a long region of muddy bed. As a simple model the incident wave is assumed to be sinusoidally modulated before entering the mud region,

$$A(0, t_1) = A_0 \cos \Omega t_1, \tag{8.1}$$

where A_0 is the normalized wave amplitude which can be taken to be unity. It is easy to see that the surface wave amplitude for $x_1 > 0$ is

$$A(x_1, t_1) = A_0 \mathrm{e}^{\mathrm{i}k_1 x_1}\cos(Kx_1 - \Omega t_1), \quad x_1 > 0, \tag{8.2}$$

where $\Omega = KC_g$ with C_g being the group velocity of the carrier wave. The bandwidths of wavenumber and frequency are measured by ϵK and $\epsilon\Omega = \epsilon KC_g$ respectively. The limit of $K = 0$ corresponds to monochromatic waves. Equation (8.2) gives the slow evolution of the surface wave amplitude in time and space.

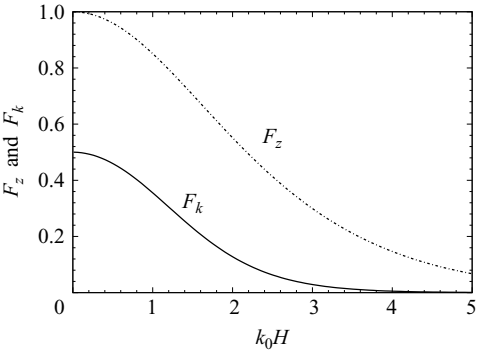

FIGURE 4. $F_k(k_0H)$ and $F_z(k_0H)$.

8.2. *Damping rate and wavenumber shift*

Since $k_1x_1 = \epsilon k_1 x$, the real part ϵk_1^r is the shift of the wavenumber per unit propagation distance, and the imaginary part $\epsilon k_1^{\mathrm{i}} = 2\pi/L$ is the local rate of spatial attenuation, which defines the distance of attenuation L. Recalling $\epsilon = \omega^2 a_0/g$, we rewrite (7.9) as

$$\frac{\epsilon k_1}{k_0} = -\gamma \frac{d_0}{h} F_k(k_0H) G(\sigma), \tag{8.3}$$

where $F_k(k_0H)$ is a real factor characterizing the wave motion in water,

$$F_k(q) = \frac{2q}{2q + \sinh(2q)} > 0, \tag{8.4}$$

and it is plotted in figure 4.

The fractional wavenumber shift and relative attenuation rate can be written as

$$\Delta k = \mathrm{Re}\left(\frac{\epsilon k_1}{k_0}\right) = -\gamma \frac{d}{h} F_k(q) \mathrm{Re}\left\{G(\sigma)\right\}, \tag{8.5}$$

$$\frac{\lambda}{L} = \mathrm{Im}\left(\frac{\epsilon k_1}{k_0}\right) = -\gamma \frac{d}{h} F_k(q) \mathrm{Im}\left\{G(\sigma)\right\}, \tag{8.6}$$

where $\lambda \equiv 2\pi/k_0$ denotes the wavelength and L the local length scale of attenuation. Thus both damping and wavenumber shift decrease exponentially with decreasing wavelength or increasing depth. As expected, mud has negligible effect on the waves for either very short waves or great water depth ($k_0H \gg 1$).

The complex factor $G(\sigma)$ defined in (6.14) embodies the effects of mud rheology. If the Stokes layer is much thinner than the mud depth, $d \gg \delta_S$ ($D \gg 1$), then $\tanh\sigma/\sigma \propto 1/D \approx 0$ and $G \approx 1$. Mud is then a thin layer of practically inviscid fluid of a different density. Attenuation is insignificant; only the wavenumber is shifted. On the other hand when mud is so viscous that $D \to 0$, $\mathrm{Re}(G), \mathrm{Im}(G) \to 0$, which leads to $G(\theta, D) \to 0$. In this limit mud does not move and hence has no effect on waves. Therefore, wave attenuation is zero when D is either very small or very large and must be the greatest for some intermediate D. Note also that for small $|\sigma|$,

$$G \sim \frac{\sigma^2}{3} \quad \text{if} \quad |\sigma| \ll 1; \tag{8.7}$$

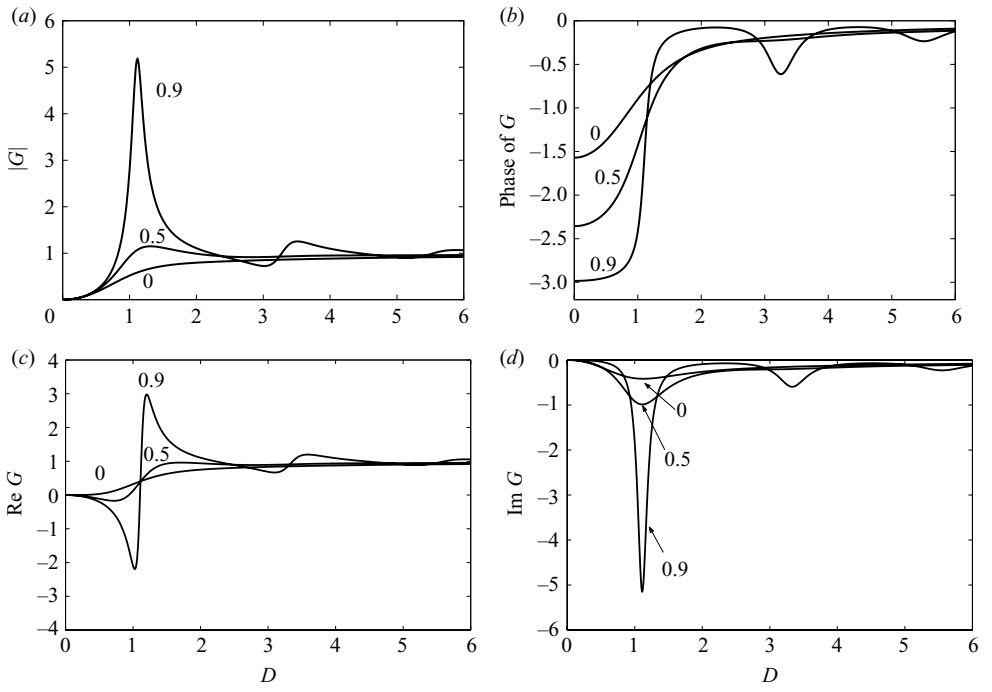

FIGURE 5. (*a*, *b*) Magnitude and phase of G. (*c*, *d*) Real and imaginary parts of G for different values of $D = \delta/\delta_S$ and the degree of elasticity $\theta \times 2/\pi = (0.0, 0.5, 0.9)$.

hence the phase of G is in the range $-\pi < \arg(G) < 0$. For large $|\sigma|$,

$$G \sim 1 - \frac{1}{\sigma} = 1 - \frac{1}{D} e^{i(\theta/2+\pi/4)} \quad \text{if} \quad |\sigma| \gg 1, \tag{8.8}$$

which is in the fourth quadrant of the complex σ plane slightly below the real axis. For intermediate values of $|\sigma|$, we use (6.16) and (6.17) to obtain

$$\tanh(\sigma) = \frac{\sinh(\beta D)\cosh(\beta D) - i\sin(\alpha D)\cos(\alpha D)}{\cos^2(\alpha D)\cosh^2(\beta D) + \sin^2(\alpha D)\sinh^2(\beta D)}. \tag{8.9}$$

The real and imaginary parts of G (figure 5), which are proportional respectively to the wavenumber shift and attenuation rate, are

$$\begin{aligned} \mathrm{Re}G &= 1 - \frac{1}{2D}[-\alpha \mathrm{Im}(\tanh\lambda) + \beta \mathrm{Re}(\tanh\lambda)] \\ &= 1 - \frac{1}{2D}\left(\frac{\alpha\sin(\alpha D)\cos(\alpha D) + \beta\sinh(\beta D)\cosh(\beta D)}{\cos^2(\alpha D)\cosh^2(\beta D) + \sin^2(\alpha D)\sinh^2(\beta D)}\right), \end{aligned} \tag{8.10}$$

$$\begin{aligned} \mathrm{Im}G &= -\frac{1}{2D}[\alpha \mathrm{Re}(\tanh\lambda) + \beta \mathrm{Im}(\tanh\lambda)] \\ &= -\frac{1}{2D}\left(\frac{\alpha\sinh(\beta D)\cosh(\beta D) - \beta\sin(\alpha D)\cos(\alpha D)}{\cos^2(\alpha D)\cosh^2(\beta D) + \sin^2(\alpha D)\sinh^2(\beta D)}\right). \end{aligned} \tag{8.11}$$

The Newtonian limits of (8.5) and (8.6) are obtained by taking $\theta = 0$,

$$\Delta k = \mathrm{Re}\left(\frac{\epsilon k_1}{k_0}\right) = -\gamma \frac{d}{h}\left(\frac{2q}{2q + \sinh(2q)}\right)\left(1 + \frac{1}{2D}\frac{\sin D\cos D + \sinh D\cosh D}{\cos^2 D\cosh^2 D + \sin^2 D\sinh^2 D}\right), \tag{8.12}$$

$$\frac{\lambda}{L} = \mathrm{Im}\left(\frac{\epsilon k_1}{k_0}\right) = \gamma \frac{\delta_S}{h}\left(\frac{q}{2q + \sinh(2q)}\right)\left(\frac{\sinh D\,\cosh D - \sin D\cos D}{\cos^2 D\cosh^2 D + \sin^2 D\sinh^2 D}\right), \tag{8.13}$$

which agree with the result of Ng (2000) if the water viscosity is ignored.

Note from (8.9) that the denominator of $G(\theta, D)$ vanishes if

$$\cos(\alpha D) = \sinh(\beta D) = 0, \tag{8.14}$$

i.e. when

$$\theta = \frac{\pi}{2}, \quad D = \left(\frac{1}{2} + m\right)\frac{\pi}{\sqrt{2}}, \quad \text{where } m \text{ is an integer.} \tag{8.15}$$

Thus large amplification signifies resonance and may occur if the mud is highly elastic ($\theta \sim \pi/2$) and if the ratio of the mud-layer depth to its Stokes' boundary-layer thickness has the special value given by (8.15). In particular the first few peaks of $|G|$ are at $D = 1.11, 3.33, 5.55$ for $m = 0, 1, 2$. Since with increase in $k_0 H$, $D = d/\delta_S$ increases monotonically and the wave factors $F_z(k_0 H)$ and $F_k(k_0 H)$ decay exponentially, only the first value, $D = 1.11$, can lead to significant interface displacement and damping.

8.3. *Interface displacement*

From (6.13) we obtain the ratio of the interface amplitude to the surface wave amplitude,

$$R = |R|\mathrm{e}^{\mathrm{i}\theta_R} \equiv \frac{\zeta'_{01}}{\eta'_{01}} = \frac{\epsilon\zeta_{01}}{A} \equiv \gamma\frac{d}{h}\frac{q}{\sinh q}\left(1 - \frac{\tanh\sigma}{\sigma}\right) = \gamma\frac{d}{h}F_z(k_0 H)G(\sigma). \tag{8.16}$$

The factor

$$F_z(k_0 H) = \frac{k_0 H}{\sinh(k_0 H)} \tag{8.17}$$

represents solely the water-wave properties; it decreases exponentially for large water depth, as also shown in figure 4.

8.4. *Numerical results of first-order predictions*

In this section, we present the relative displacement of the interface according to (8.16) and the damping rate and the wavenumber shift for both Hangzhou Bay mud and Lianyungang mud. Several mud concentrations and mud-layer thicknesses are examined for fixed water depth $h = 10$ m.

8.4.1. *Interface displacement*

Results for Hangzhou Bay mud are presented in figure 6. One can see that for shorter water waves the interface and the free surface are more in phase with each other. Owing to the relatively weak elasticity, the interface displacement is at most a few per cent that of the free surface, for mud depth no greater than 10 % of the water depth. Results for unlikely deep mud layer with $d/h = 0.2$ show a greater interface amplitude. As expected, higher mud concentration is associated with smaller interface displacement.

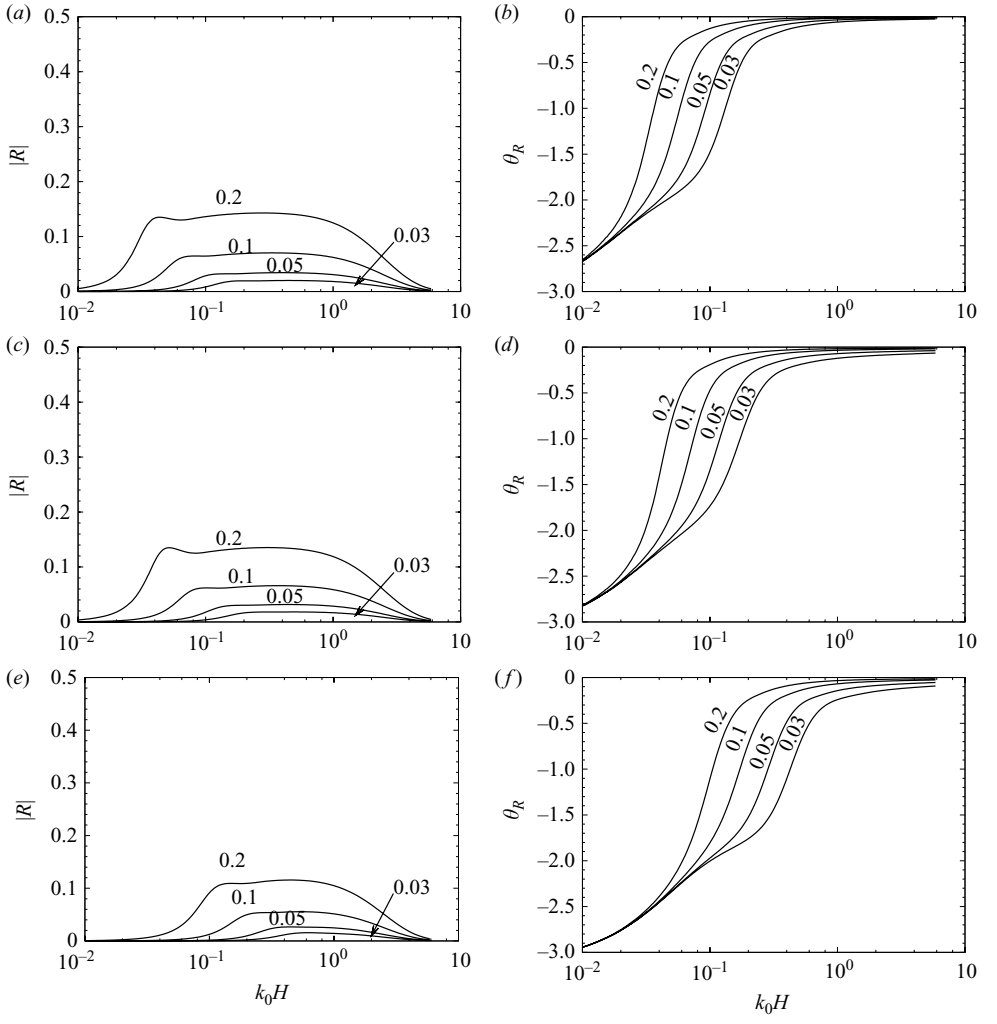

FIGURE 6. Modulus and phase of the ratio of complex vertical displacements $R = \epsilon\zeta_{10}/A$ for Hangzhou Bay mud samples: (*a*, *b*) $\phi = 0.20$; (*c*, *d*) $\phi = 0.24$; (*e*, *f*) $\phi = 0.34$.

Interface displacements for Lianyungang mud are shown in figure 7. For the smallest concentration ($\phi = 0.17$) and a sufficiently deep mud layer with $d/h = 0.1$, the interface displacement can be as high as 15 % of the free-surface displacement. For the unlikely deep mud with $d/h = 0.2$ the interface displacement can be as high as 45 % of that of the free surface. This is clearly due to the high elasticity which permits relatively strong resonance. Again, higher concentration leads to smaller interface motion.

8.4.2. *Damping rate and wavenumber shift*

The damping rate and the wavenumber shift for Hangzhou Bay mud are shown in figures 8. Note that as the concentration increases the maximum (resonant) damping decreases and the waves become longer. This is because the mud movement is reduced with increase in concentration. For the same reason damping increases, and wavelength increases with the mud depth.

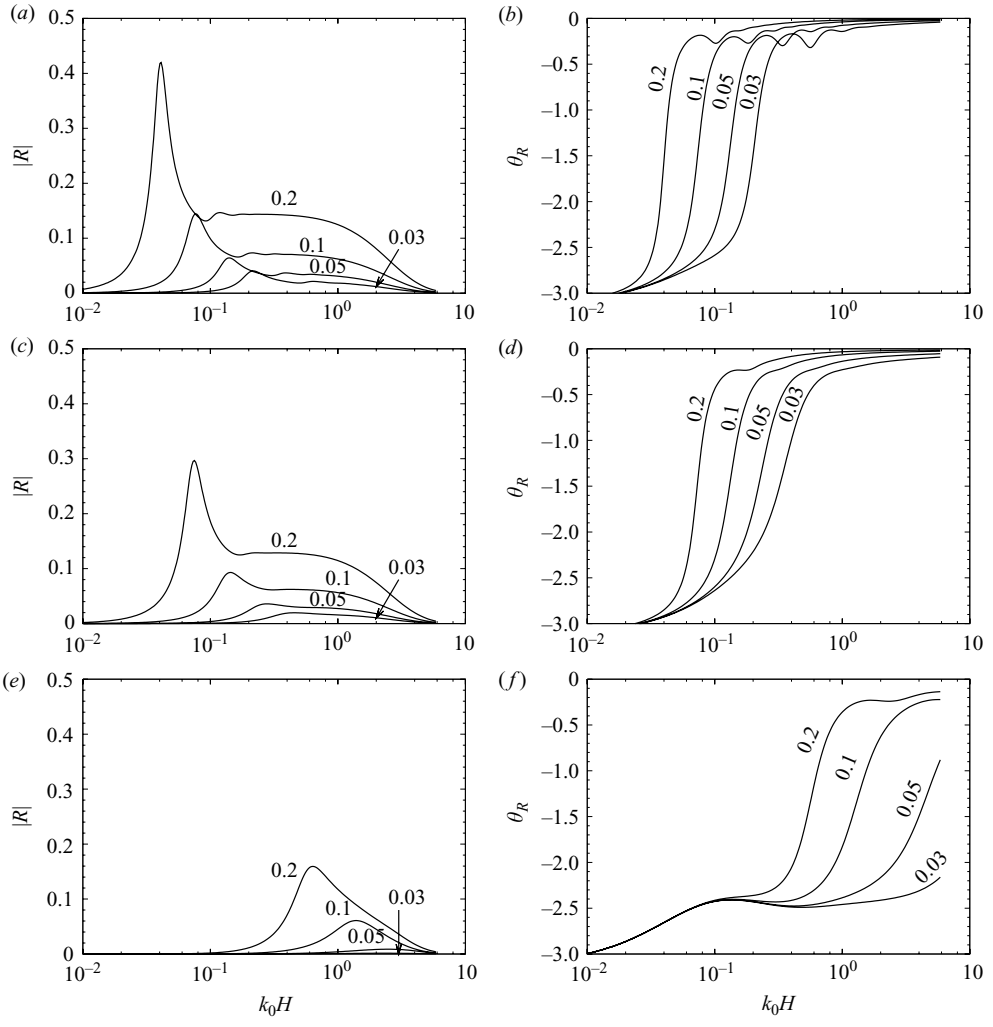

FIGURE 7. Modulus and phase of the ratio of complex vertical displacements R for Lianyungang mud sample: (a, b) $\phi = 0.17$; (c, d) $\phi = 0.26$; (e, f) $\phi = 0.50$.

We now turn to the results for Lianyungang mud which has much larger viscoelastic coefficients. The damping rate and wavenumber shift are plotted for three solid concentrations in figure 9 for depth ratios $d/h = 0.03,\ 0.05,\ 0.1,\ 0.2$. Again when the solid volume fraction increases, the interface moves less; hence the damping rate decreases and the wavenumber further reduces. The resonant peaks are shifted to shorter wavelengths (larger k_0H). For large k_0H the wavenumber shift become increasingly positive, and the wavelengths tend to become shorter.

9. Infragravity waves

It is well known in the classical theory of waves over a rigid bottom that radiation stresses in narrow-banded short waves force set-down and infragravity waves of long periods and wavelengths (Longuet-Higgins & Stewart 1964). Without strong reflection

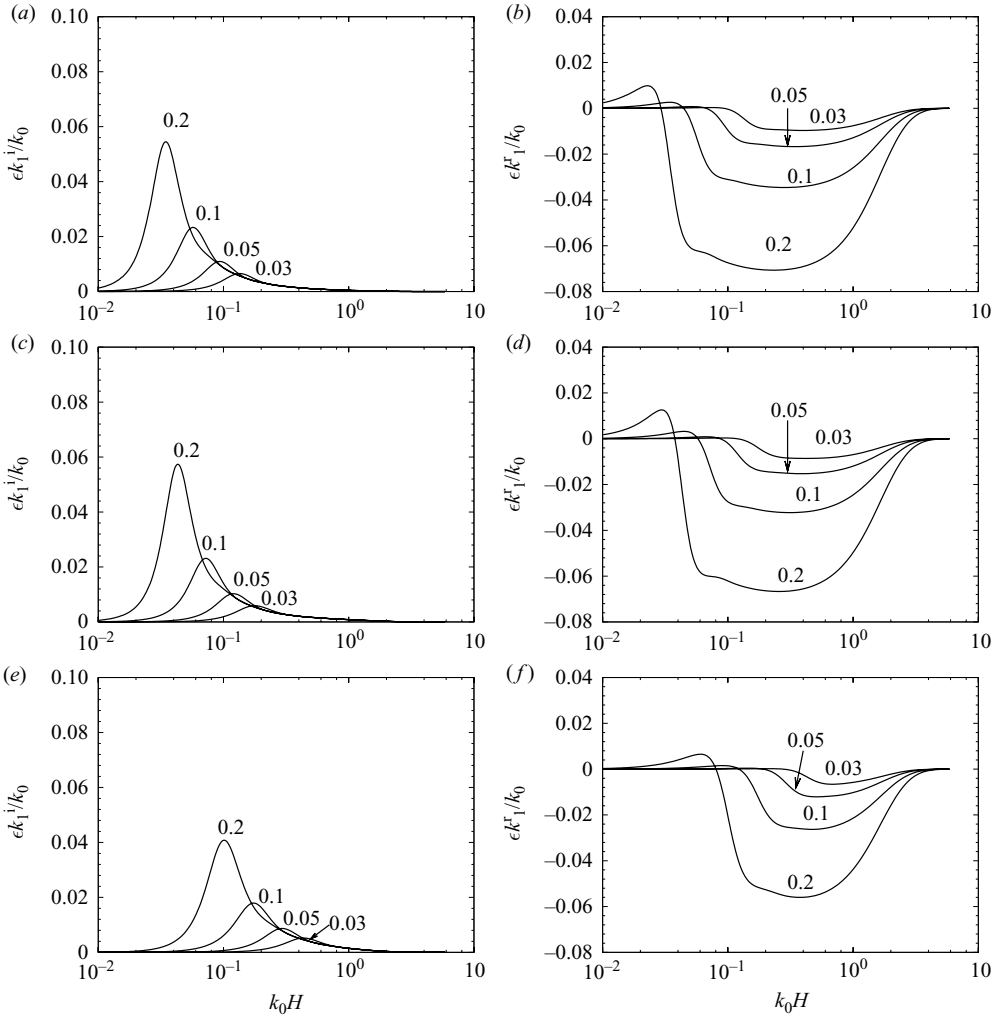

FIGURE 8. Damping coefficient $\epsilon k_1^i/k_0$ and wavenumber shift $\epsilon k_1^r/k_0$ for Hangzhou Bay mud: (*a*, *b*) $\phi = 0.20$; (*c*, *d*) $\phi = 0.24$; (*e*, *f*) $\phi = 0.34$

the long wave propagates with the envelope of the short waves and is called the bound long wave.

With reference to (5.4), (5.5) and (5.7), the forcing function F_{20} and G_{20} are formally the same as those for a rigid seabed:

$$F_{20} = -g\frac{\partial^2 \Phi_{00}}{\partial x_1^2}, \tag{9.1}$$

$$G_{20} = \frac{k_0}{2}\frac{\partial |A|^2}{\partial x_1} - \frac{1}{4\sinh^2 q}\frac{\partial |A|^2}{\partial t_1} - \frac{\partial \Phi_{00}}{\partial t_1}, \tag{9.2}$$

$$L_{20} = \frac{\partial \zeta_{00}}{\partial t_1} = 0. \tag{9.3}$$

The interface velocity vanishes trivially ($L_{20} = 0$) since $\zeta_{00} = 0$. Therefore the equation governing the long-wave potential remains the same as if the bed were rigid without

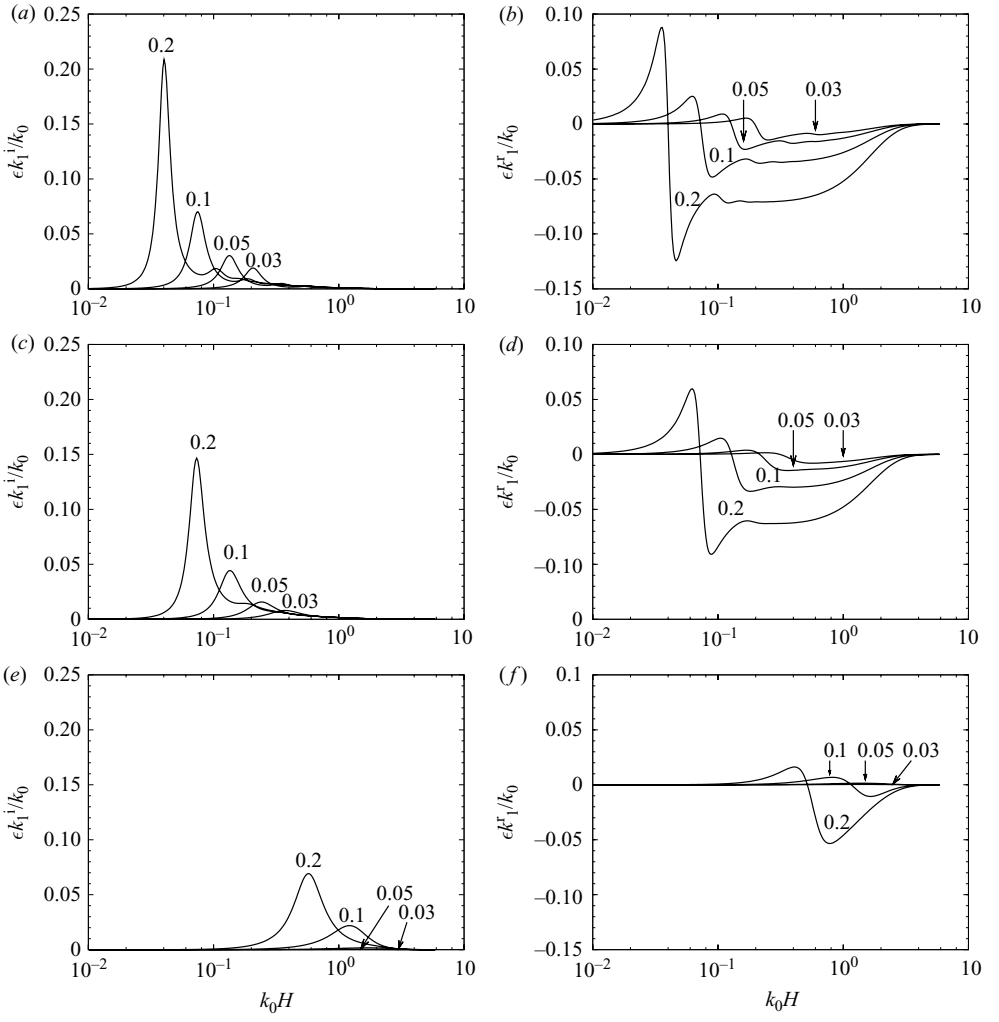

FIGURE 9. Damping coefficient $\epsilon k_1^{\mathrm{i}}/k_0$ and wavenumber shift $\epsilon k_1^{r}/k_0$ for Lianyungang mud: (a, b) $\phi = 0.17$; (c, d) $\phi = 0.26$ (e, f) $\phi = 0.50$.

mud (see Mei 1989),

$$\frac{\partial^2 \Phi_{00}}{\partial t_1^2} - H\frac{\partial^2 \Phi_{00}}{\partial x_1^2} = \frac{k_0}{2}\frac{\partial |A|^2}{\partial x_1} - \frac{1}{4\sinh^2 q}\frac{\partial |A|^2}{\partial t_1}. \tag{9.4}$$

However, mud motion influences the long (infragravity) wave indirectly through the slow variation of A governed by (7.7).

In the muddy region, the forcing term on the right-hand side of (9.4) is

$$\begin{aligned}
&\frac{\mathrm{i}k_0 K}{4}A_0^2\left\{2\mathrm{i}\frac{k_1^{\mathrm{i}}}{K}e^{-2k_1^{\mathrm{i}}x_1} + \left[1 + \mathrm{i}\frac{k_1^{\mathrm{i}}}{K} + \frac{C_g}{\sinh(2k_0H)}\right]\mathrm{e}^{2\mathrm{i}[(K+\mathrm{i}k_1^{\mathrm{i}})x_1 - \Omega t_1]}\right.\\
&\qquad\left. - \left[1 - \mathrm{i}\frac{k_1^{\mathrm{i}}}{K} + \frac{C_g}{\sinh(2k_0H)}\right]\mathrm{e}^{-2\mathrm{i}[(K-\mathrm{i}k_1^{\mathrm{i}})x_1 - \Omega t_1]}\right\}\\
&\quad = \mathrm{i}\mathscr{P}A_0^2\mathrm{e}^{-2k_1^{\mathrm{i}}x_1}\left\{2\mathrm{i}\mathscr{Q} + [1 + \mathrm{i}\mathscr{Q}]\,\mathrm{e}^{2\mathrm{i}[Kx_1 - \Omega t_1]} - [1 - \mathrm{i}\mathscr{Q}]\,\mathrm{e}^{-2\mathrm{i}[Kx_1 - \Omega t_1]}\right\}
\end{aligned} \tag{9.5}$$

with the real parameters

$$\mathscr{P} = \frac{k_0 K}{4}\left(1 + \frac{C_g}{\sinh(2k_0 H)}\right) \tag{9.6}$$

and

$$\mathscr{Q} = \frac{k_1^{\mathrm{i}}}{K}\left(\frac{1}{1 + \dfrac{C_g}{\sinh(2k_0 H)}}\right). \tag{9.7}$$

Note that

$$\frac{k_1^{\mathrm{i}}}{K} = \frac{\epsilon k_1^{\mathrm{i}}/k_0}{\epsilon K/k_0}, \tag{9.8}$$

which depends on several length ratios (d/a_0, $k_0 H$ and the relative bandwidth $\epsilon K/k_0$). The long-wave solution is easily found to be

$$\Phi_{00}(x_1, t_1) = A_0^2 \mathrm{e}^{-2k_1^{\mathrm{i}} x_1}\left[\frac{\mathscr{P}\mathscr{Q}}{2H\left(k_1^{\mathrm{i}}\right)^2} + \left(\frac{\mathrm{i}\mathscr{R}^*\mathscr{P}}{4K^2\left(H - C_g^2\right)}\mathrm{e}^{2\mathrm{i}[Kx_1 - \Omega t_1]} + \text{c.c.}\right)\right]. \tag{9.9}$$

The complex parameter $\mathscr{R}$ is defined by

$$\mathscr{R} = \frac{1 - \mathrm{i}\mathscr{Q}}{1 - 2\mathrm{i}\dfrac{H}{H - C_g^2}\dfrac{k_1^{\mathrm{i}}}{K} - \dfrac{H}{H - C_g^2}\left(\dfrac{k_1^{\mathrm{i}}}{K}\right)^2}, \tag{9.10}$$

which depends on wave and mud properties.

From the long-wave potential (9.9) the mean horizontal velocity ϵU is derived:

$$U = \frac{\partial \Phi_{00}}{\partial x_1} = \langle U\rangle + \mathrm{Re}(\widetilde{U}\mathrm{e}^{2\mathrm{i}(Kx_1 - \Omega t_1)}), \tag{9.11}$$

where Re stands for 'real part of' and $\langle U\rangle$ for the steady current,

$$\langle U(x_1)\rangle = \epsilon\frac{\partial \Phi_{00}}{\partial x_1} = -\mathrm{e}^{-2k_1^{\mathrm{i}} x_1}\frac{2k_1^{\mathrm{i}}\mathscr{P}\mathscr{Q}}{2H\left(k_1^{\mathrm{i}}\right)^2} = -\frac{k_0 A_0^2}{4H}\mathrm{e}^{-2k_1^{\mathrm{i}} x_1}, \tag{9.12}$$

which is in the direction opposite to the waves and diminishes forward as the waves are damped. This return current is the consequence of requiring the net mass flow to be zero, possibly because of the presence of a wall at $x \sim +\infty$, and can also be derived from mass conservation:

$$\left\langle \overline{\int_{-H}^{\epsilon\eta} u\,\mathrm{d}z} \right\rangle = 0, \quad \text{i.e.} \quad \epsilon\langle U\rangle H + \epsilon\left\langle \int_{-H}^{0} \overline{\eta u_0}\,\mathrm{d}z \right\rangle + O(\epsilon^2) = 0, \tag{9.13}$$

where the overline denotes the wave-period (short-time) average. Therefore,

$$\langle U\rangle = -\frac{1}{H}\left\langle \int_{-H}^{0} \overline{\eta u_0}\,\mathrm{d}z \right\rangle, \tag{9.14}$$

which gives the same result as (9.12). It should be noted that any uniform current is a solution to (9.4) and can be added to the current above. The magnitude can only be determined by imposing the boundary condition at either infinity. The velocity

amplitude of the bound long wave is

$$\widetilde{U} = -\frac{k_0 A_0^2}{4} \frac{1 + \dfrac{C_g}{\sinh 2k_0 H}}{\left(H - C_g^2\right)} \mathscr{R}^* \left(1 + \mathrm{i}\frac{k_1^{\mathrm{i}}}{K}\right) \mathrm{e}^{-2k_1^{\mathrm{i}} x_1}. \tag{9.15}$$

In the limit of no mud, $R = 1, k_1^{\mathrm{i}} = 0$; then the horizontal velocity of the bound wave over the rigid bed (denote by the subscript 'RB') has the amplitude of the classical result owing to Longuet-Higgins & Stewart (1964),

$$\widetilde{U}_{RB} = -\frac{k_0 A_0^2}{4} \frac{1 + \dfrac{C_g}{\sinh 2k_0 H}}{\left(H - C_g^2\right)}, \tag{9.16}$$

which is independent of the bandwidth K. We note that in shallow water

$$H = \frac{1}{k_0^2}\left(1 + \frac{(k_0 H)^2}{3} + \cdots\right), \quad C_g = \frac{1}{k_0}\left(1 - \frac{(k_0 H)^2}{3} + \cdots\right)$$

from (5.10) and (7.8) for $k_0 H \ll 1$, so that $H - C_g^2 \sim 1/(k_0 H)^4$ becomes unbounded. In shallow water, (9.16) derived by Stokes' expansion loses validity and must be replaced by Boussinesq's approximation, as is well known.

Let us rewrite (9.15) as

$$\tilde{U} = \Psi U_{RB}\, \mathrm{e}^{-2k_1^{\mathrm{i}} x_1}, \text{ where } \Psi = \mathscr{R}^* \left(1 + \mathrm{i}\frac{k_1^{\mathrm{i}}}{K}\right). \tag{9.17}$$

With the help of (9.8), the dependence of the ratio $|\Psi|$ on $\epsilon K/k_0$ is shown for the two mud samples and two concentrations in figures 10 and 11. Note that for all mud concentrations, $|\Psi| \approx 1$ when $k_0 H > 1$. In intermediate depths the bound long wave is still affected by mud and attenuates with distance. For $k_0 H \to 0$, (9.17) is no longer valid, although it can be shown that $|\Psi| \to 1$. As the mud concentration increases, $|\Psi|$ is closer to unity. This is particularly so for the heavy and shallow mud in Lianyungang with $\phi = 0.50$ and $d/h = 0.05$, which is hardly moved by the short wave and hence does not modify the bound long wave.

The mean sea level η_{10} is deduced from Φ_{00} according to (7.3):

$$\eta_{10} = \langle \eta \rangle + \mathrm{Re}\left(N\, \mathrm{e}^{-2k_1^{\mathrm{i}} x_1}\, \mathrm{e}^{2\mathrm{i}K(x_1 - C_g t_1)}\right), \tag{9.18}$$

where the first term is the steady-state set-down,

$$\langle \eta \rangle = -\frac{A_0^2}{8 \sinh^2 k_0 H} \mathrm{e}^{-2k_1^{\mathrm{i}} x_1}, \tag{9.19}$$

which increases monotonically from the largest negative value (set-down) at the initial station, $x_1 = 0$, to zero at sufficiently large x_1 when short waves are damped out. The second term represents the bound long wave of amplitude N where

$$N = -\frac{A_0^2}{4} \left\{ \frac{k_0 C_g \left(1 + \mathrm{i}\dfrac{k_1^{\mathrm{i}}}{K} + \dfrac{C_g}{\sinh 2k_0 H}\right)}{H\left(1 + \mathrm{i}\dfrac{k_1^{\mathrm{i}}}{K}\right)^2 - C_g^2} + \frac{k_0^2}{2\cosh^2 k_0 H} \right\}. \tag{9.20}$$

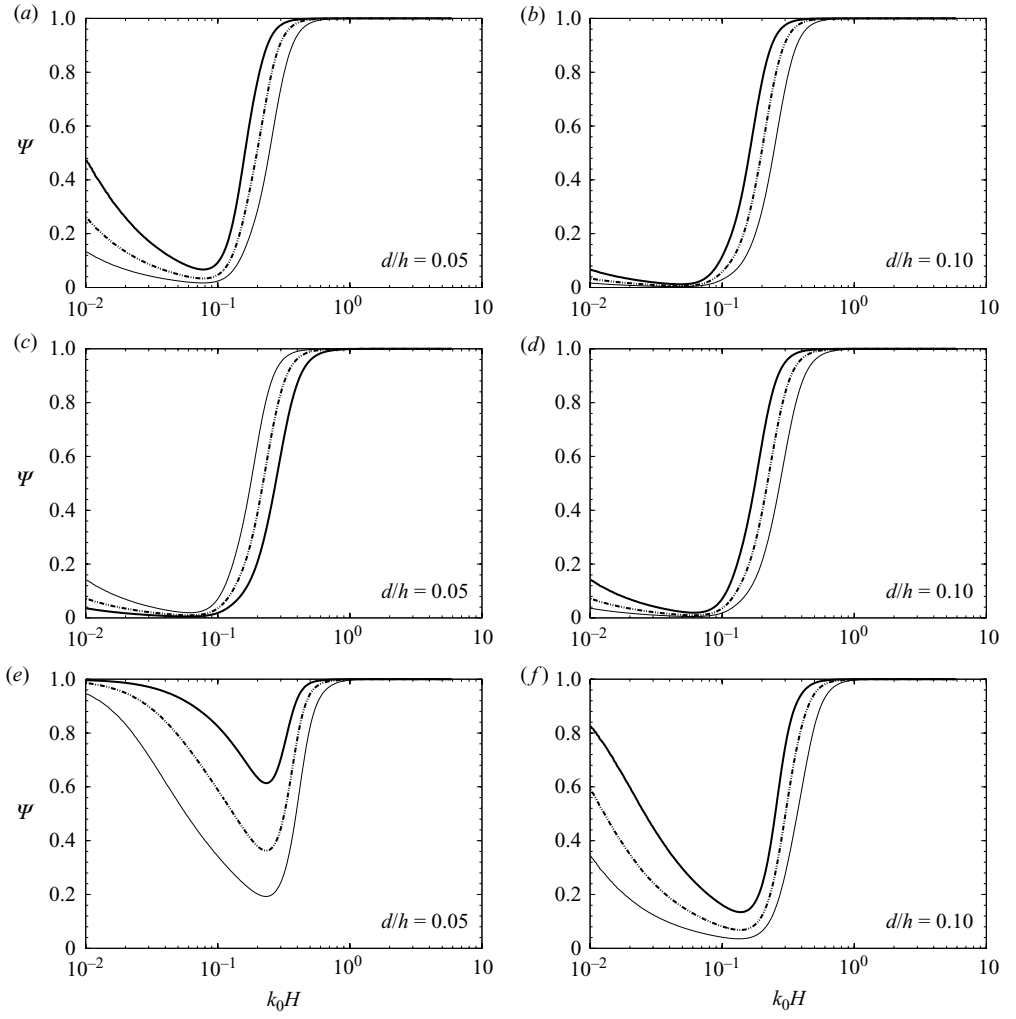

FIGURE 10. Factor Ψ of bound long wave for Hangzhou Bay mud: (*a*, *b*) $\phi = 0.20$; (*c*, *d*) $\phi = 0.24$; (*e*, *f*) $\phi = 0.34$. The thick solid line represents $\epsilon K/k_0 = 0.2$; the chain represents $\epsilon K/k_0 = 0.1$; the thin solid line represents $\epsilon K/k_0 = 0.05$.

If there is no mud ($k_1^{\mathrm{i}}/K = 0$), the seabed is rigid; the bound-long-wave amplitude after using the dispersion relation (5.10) and the group velocity (7.8) is

$$\left.\begin{aligned} N_{RB} &= -\frac{A_0^2}{4}\left\{k_0 C_g \frac{1+\dfrac{C_g}{\sinh 2k_0 H}}{H - C_g^2} + \frac{k_0^2}{2\cosh^2 k_0 H}\right\} \\ &= -\frac{A_0^2}{4\left(H - C_g^2\right)}\left\{k_0 C_g\left(1 + \frac{C_g}{\sinh 2k_0 H}\right) + \frac{k_0\left(H - C_g^2\right)}{\sinh 2k_0 H}\right\} \\ &= -\frac{A_0^2}{4\left(H - C_g^2\right)}\left(2k_0 C_g - \frac{1}{2}\right). \end{aligned}\right\} \tag{9.21}$$

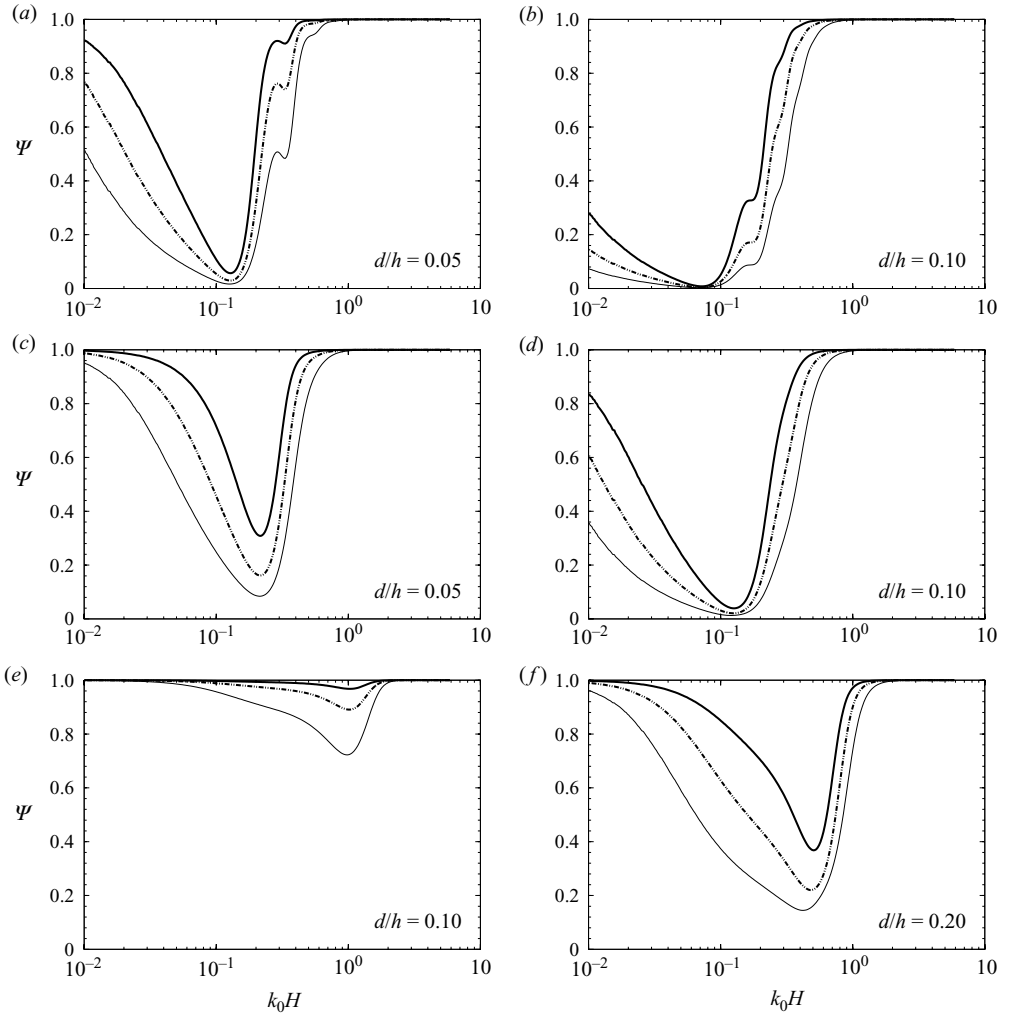

FIGURE 11. Factor Ψ of bound long wave for Lianyungang mud: (*a*, *b*) $\phi = 0.17$ for $d/h = 0.05, 0.1$; (*c*, *d*) $\phi = 0.26$ for $d/h = 0.05, 0.10$; (*e*, *f*) $\phi = 0.50$ for $d/h = 0.1, 0.2$. For the densest mud with $d/h = 0.05$, $|\Psi| \approx 1$ for all $k_0 H$ and is not plotted. The thick solid line represents $\epsilon K/k_0 = 0.2$; the chain represents $\epsilon K/k_0 = 0.1$; the thin solid line represents $\epsilon K/k_0 = 0.05$.

In dimensional terms, the last expression is

$$N'_{RB} = -\frac{A_0'^2}{4\left(gh - C_g'^2\right)}\left(\frac{2C'_g}{C'} - \frac{1}{2}\right), \tag{9.22}$$

which is the classical result of Longuet-Higgins & Stewart (1964).

Let us rewrite (9.20) as

$$N = \Pi N_{RB} \mathrm{e}^{-2k_1^i x_1}, \tag{9.23}$$

where

$$\Pi = \left| \left(\frac{k_0 C_g \left(1 + \mathrm{i}\dfrac{k_1^{\mathrm{i}}}{K} + \dfrac{C_g}{\sinh 2k_0 H}\right)}{H\left(1 + \mathrm{i}\dfrac{k_1^{\mathrm{i}}}{K}\right)^2 - C_g^2} + \frac{k_0^2}{2\cosh^2 k_0 H} \right) \frac{\left(H - C_g^2\right)}{\left(2k_0 C_g - \dfrac{1}{2}\right)} \right|. \tag{9.24}$$

The behaviour of Π on $\epsilon K/k_0$ and $k_0 H$ for the mud samples from two field sites is very close to that of Ψ and is not plotted here.

In addition to the low-frequency wave, second-harmonic short waves are also present and contribute to the free-surface height at the second order, i.e. $O(\epsilon)$, given by (7.13)–(7.15). It is evident that the amplitude of the second-harmonic decays in half of the distance as the first.

10. Concluding remarks

We have derived an approximate theory for the propagation of narrow-banded surface waves over a thin horizontal layer of fluid mud at the sea bed. Since typical viscosity of mud is far greater than that of water, we treat water as inviscid. The fluid mud is modelled as a viscoelastic material with a frequency-dependent complex viscosity. At the first order, analytical expressions of interface displacement, wave attenuation and wavenumber shifts are found and discussed. It is found that the mud motion can be significantly enhanced by resonance if the mud elasticity is strong and the mud layer is relatively thick. Second-order effects of mean set-down and bound long waves are examined. Owing to attenuation of short waves the second-order set-down diminishes with the distance of wave propagation and induces a reverse current that increases in strength in the backward direction. The amplitude of the bound long wave is smaller for higher concentration and larger bandwidth. The second harmonic also decays with distance twice as fast as the first-harmonic primary waves. In very shallow water, the present (Stokes) theory breaks down.

Extensions to gradually decreasing water depth and broad-banded random waves will be of practical interest. Accounting for strong nonlinearity by Boussinesq approximation to avoid the breakdown of Stokes expansions is needed, as in Liu & Chan (2007) who modelled the mud layer as a Newtonian fluid. Mass transport (induced streaming) and other second-order effects in the mud layer can be carried out by advancing the mud dynamics to $O(\epsilon)$. Since the long-scale motion corresponds to low frequencies, one should start from the general constitutive law (2.2) instead of (2.1) and apply the multiple-scale analysis. In nature, fluid mud is only the upper layer mobilized from an initially consolidated soil of much higher density and little fluidity. It is of fundamental importance to predict the depth and the density variation of the mobile layer. This is an immense challenge in the fluid dynamics of sediment transport.

This research was funded by US Office of Naval Research as a part of the Multidisciplinary University Research Initiative (MURI) programme under grant N00014-06-1-0718.

REFERENCES

Coussot, P. 1997 *Mud Flow Rheology and Dynamics*. Bakema.

Dalrymple, R. & Liu, P. L.-F. 1978 Waves over soft muds: a two-layer fluid model. *J. Phys. Oceanogr.* **8** (6), 1121–1131.

Foda, M. A., Hunt, J. R. & Chou, H. T. 1993 A nonlinear model for the fluidization of marine mud by waves. *J. Geophys. Res* **98**, 7039–7047.

Hsiao, S. V. & Shemdin, O. H. 1980 Interaction of ocean wave with a soft bottom. *J. Phys. Oceanogr*. **10**, 605–610.

Huang, Z., Huhe, A. & Zhang, Y. 1992 An experimental study of the properties of fluid mud in Xishu, Lianyungang. *Tech Rep*. IMCAS STR-92019. Institute of Mechanics, Chinese Academy of Sciences. In Chinese.

Huhe, A. & Huang, Z. H. 1994 An experimental study of fluid mud rheology – mud properties in Hangzhou Bay navigation channel. Part II. Beijing. Rep. No. 1. Institute of Mechanics, Chinese Academy of Sciences, pp. 34–56. In Chinese.

Jiang, F. & Mehta, A. J. 1995 Mudbanks of the southwest coast of India. Part IV. Mud viscoelastic properties. *J. Coastal Res*. **11** (3), 918–926.

Liu, K. F. & Mei, C. 1989 Effects of wave-induced friction on a muddy seabed modelled as a Bingham-plastic fluid. *J. Coastal Res*. **5** (4), 777–789.

Liu, P. L.-F. & Chan, I.-C. 2007 On long-wave propagation over a fluid-mud seabed. *J. Fluid Mech*. **579**, 467–480.

Longuet-Higgins, M. S. & Stewart, R. W. 1964 Radiation stresses in water waves, a physical discussion with applications. *Deep-Sea Res*. **11**, 529–562.

Maa, J. P.-Y. & Mehta, A. J. 1988 Soft mud properties: Voigt model. *J. Waterways Port Coastal Ocean Engng* **114** (6), 765–770.

MacPherson, H. 1980 The attenuation of water waves over a non-rigid bed. *J. Fluid Mech*. **97**, 721–742.

Malvern, L. E. 1969 *Introduction to the Mechanics of a Continuous Medium*. Prentice Hall.

Mei, C. C. 1989 *The Applied Dynamics of Ocean Surface Waves*. World Scientific.

Ng, C. 2000 Water waves over a muddy bed: a two-layer Stokes' boundary layer model. *J. Coastal Engng* **40**, 221–242

Ng, C. & Zhang, X. 2007 Mass transport in water waves over a thin layer of soft viscoelastic mud. *J. Fluid Mech*. **573**, 105–130.

Piedra-Cueva, I. 1993 On the response of a muddy bottom to surface water waves. *J. Hydraul. Res*. **31**, 681–695.

Shibayama, T., Okuno, M. & Sato, S. 1990 Mass transport rate in muddy layer due to wave action. In *Proceedings of the 22nd Coastal Engineering Conference* (ed. B. L. Edge), pp. 3037–3049. ASCE.

Soltanpour, M., Shibayama, T. & Noma, T. 2003 Cross-shore mud transport and beach deformation mode. *J. Coastal Engng* **45**, 363–386.

Wan, Z. H. & Wang, Z. Y. 1994 *Hyperconcentrated Flow*. Balkema.

de Wit, P. J & Kranenburg C. 1997 On the liquefaction and erosion of mud due to waves and current. In *Proceedings of INTERCOH '94* (ed. J. Watts, N. Burt & R. Parker), pp. 331–340.

Zhang, X. & Ng, C. O. 2006 On the oscillatory and mean motions due to waves in a thin viscoelastic layer. *Wave Mot*. **43**, 387–405.